RSC Advances

ROYAL SOCIETY OF CHEMISTRY

www.rsc.org/advances

Enhancement of N_2O catalytic decomposition over Ca modified Co_3O_4 catalyst

Qiulin Zhang, Xiaosu Tang, Ping Ning *, Yankang Duan, Zhongxian Song, Yuzhen Shi,

Faculty of Environmental Science and Engineering, Kunming University of Science and Technology. Kunming, 650500, P.R. China

E-mail: qiulinzhang_kmust@163.com ningping58@sina.com

Abstract: A series of Ca modified Co_3O_4 catalysts with different Ca/Co molar ratios were synthesized by the co-precipitation method and applied to the N_2O catalytic decomposition. The experimental results showed that the performance of N_2O catalytic decomposition was obviously enhanced by the addition of Ca into the Co_3O_4 catalyst. The Ca modified Co_3O_4 catalyst with Ca/Co molar ratio of 1:2 exhibited the highest catalytic performance and almost 100% N_2O conversion was achieved at 400 °C. The characterization results showed that the addition of proper calcium composition could promote the growth of 111 crystal plane of Co_3O_4 and provide abundant surface oxygen on the surface of catalyst. The kinetics studies confirmed that the activation energy of Ca modified Co_3O_4 catalyst with Ca/Co molar ratio of 1:2 (Ea=17.84kJ/mol) was lower than that of pure Co_3O_4 (Ea=43.21 kJ/mol), implying that the addition of Ca into the Co_3O_4 is beneficial to the catalytic decomposition of N_2O.

* Corresponding author. E-mail: *qiulinzhang_kmust@163.com*

Key words: N_2O; Catalytic decomposition; Co_3O_4; $CaCO_3$

1. Introduction

Nitrous oxide (N_2O) is a trace component of the troposphere with a lifetime of 131 years, and its concentration is increasing by 0.2-0.3% yearly.[1] Nitrous oxide (N_2O) is regarded as a major environmental pollutant since it could largely contribute to the greenhouse effect and the stratospheric ozone destruction.[2,3] N_2O is regard as the third most important greenhouse gas after CO_2 and CH_4.[4] Due to its continuously

increasing concentrations and long residence time in the atmosphere, the catalytic removal of N_2O attracts extensive attention.[5,6]

Various methods were employed for abatement of N_2O emission. Among these approaches, direct catalytic decomposition of N_2O to nitrogen and oxygen is considered as one of the most economical and effective method. Nowadays, various types of catalysts have been used for catalytic decomposition of N_2O, such as noble metals supported systems,[7-9] pure and mixed metal oxides,[10,11] and ion exchanged zeolites.[12-14] Although the noble metal catalysts exhibited excellent catalytic performance, the application of such catalysts are considerably limited by its high cost. The ion exchanged zeolites catalysts also have many limitations, they could be largely deactivated in the presence of excess oxygen and water steam.[15] However, Among the metal oxides, cobalt-based catalysts containing Co_3O_4 spinel presented high catalytic performance.[16-19] Since Co_3O_4 presented relatively high redox character, it was proved to be active for the decomposition of N_2O.[20] The N_2O catalytic decomposition activity of Co_3O_4 can be improved by different kinds of modification, such as the partial replacement of Co^{2+} by Ni^{2+}, Zn^{2+}, Mg^{2+} and Fe^{2+} over Co_3O_4 spinel oxide.[17,19,21] The rare earth (Ce, La) was proposed as the component could promote the catalytic activity of Co_3O_4 spinel by increasing the specific area and redox properties.[22] It was reported that the alkali promoter (using K_2CO_3 precursor) showed higher catalytic activities than that of pure Co_3O_4, since potassium can facilitate the activation of N_2O and promote the recombination of surface oxygen.[23] However, the potassium that existed in the catalysts would outflow easily under the water steam condition.

Among the alkaline earth metals, calcium was considered as an attractive catalytic material for its low price and almost nontoxic property.[24] It is suggested by the previous literature that the catalytic performance could be improved after Co_3O_4 impregnated with calcium.[10] In this work, the Ca modified Co_3O_4 catalyst with different molar ratio were prepared by the co-precipitation method. The effect of the addition of $CaCO_3$ into Co_3O_4 on the N_2O decomposition was studied. The XRD, H_2-TPR, XPS and TEM techniques were employed to investigate the

activity-structure relationship of $CaCoO_x$ catalyst.

2. Experiment

2.1 Catalysts preparation

The catalysts were prepared using the co-precipitation method described below. The known amounts of cobalt nitrate and calcium nitrate were dissolved in distilled water. Then 15 wt % K_2CO_3 solution was added dropwise into the obtained solution at room temperature until the pH reached 9. After 30 min stir, the solution was aged for 3h. The resultant precipitate was collected by filtration and washed with distilled water until the pH of the filtrate reached 7. The cake was dried overnight at the temperature of 100 °C, and then calcined in air at the temperature of 500 °C for 2 h. The obtained catalysts were denoted as CaxCoy (x/y=1:1, 1:2, 1:3, 1:5, which x/y represents the molar ratio of Ca/Co), Co_3O_4, $CaCO_3$.

2.2. Catalysts characterization

Powder X-ray diffraction (XRD) pattern were measured on Bruker D8 Advance X-ray diffraction meter (Germany), which are equipped with the CuKa radiation and operated at 40 kV and 40 mA. Diffraction patterns were recorded in a 2θ range between 10° and 90°.

X-ray photoelectron spectroscopy (XPS) experiments were carried out on an ULVAC PHI 5000 Versa Probe - Ⅱ equipment (Japan). All the electron binding energys were referenced to the C1s peak at 284 eV.

TEM and high resolution TEM (HRTEM) of the catalyst samples were measured on FEI Tecnai G220 transmission electron microscope, which use an accelerating voltage of 200 kV.

H_2-Temperature programmed reduction (H_2-TPR) was carried out on gas chromatography equipped with a quartz reactor and TCD detector. Before the test, 30mg samples were pretreated at 400 °C for 40min in N_2 (30 ml/min), and then cooled to 100 °C in N_2. The TPR analysis were performed under a 5% H_2/Ar (30 ml/min) using a heating rate of 10 °C/min until the temperature reached to 550 °C.

Oxygen-Temperature programmed desorption (O_2-TPD) was performed on gas chromatography equipped with a quartz reactor and TCD detector. Before the TPD

experiments, the catalysts (270mg) were pretreated at 400 °C for 1 h in He (20 ml/min), and then the sample was cooled to 120 °C in He (20 ml/min). O_2 adsorption was performed in 4% O_2/N_2 (20 ml/min) for 1h at the temperature of 120 °C for removal of physical adsorption. Then, the sample was heated from 120°C to 600 °C at a heating rate of 10 °C/min in He (20ml/min).

2.3. Catalytic measurements of N_2O decomposition

The catalytic activity measurement was carried out in a fixed-bed quartz flow reactor (6 mm i.d.) at the atmospheric pressure, and 0.2 ml (40 - 60 mesh) catalyst was used in each test. The reactant mixture was consisted of 1000 ppm N_2O, 0 or 5 vol. % O_2, 0 or 3 vol. % H_2O, Ar was used as balance gas. A total flow rate of feed gas was set at 200 ml/min, the gas hourly space velocity (GHSV) was 60,000 h^{-1}. The experiments were conducted at the temperatures between 250 °C and 500 °C in intervals of 25 °C. In order to ensure the reaction remained in steady state, the reaction temperature was kept for 30 min before each measurement. The effluent gas concentrations were analyzed by gas chromatography equipped with ECD detector. The N_2O conversion was calculated according the formula below:

$$N_2O \text{ conversion } (\%) = \frac{[N_2O]_{in} - [N_2O]_{out}}{[N_2O]_{in}} \times 100\%$$

3. Results and discussion

3.1 XRD analysis

The XRD patterns of Co_3O_4 with different calcium content were shown in **Fig.1**. As revealed by XRD patterns, the diffraction peaks for Co_3O_4 catalyst appeared at 31.23°, 36.88°, 45.03°, 59.36° and 65.21° corresponding to (111), (220), (311), (400), (511) and (440) planes of the spinel structure of Co_3O_4, respectively. No other phases, like Co_2O_3 or CoO, were found in these catalysts. In addition, the peaks belong to $CaCO_3$ (JCPDS86-0174) could also be observed on $CaCoO_x$ curves. Because of the low calcination temperature, the $Ca_9Co_{12}O_{28}$ that formed by the solid state interaction between CaO and Co_3O_4 was not observed in the XRD patterns. Compared to the diffraction peaks of the pure Co_3O_4 oxides, the diffraction peaks of Co_3O_4 for $CaCoO_x$ catalysts were weaker and broader, implying that the addition of $CaCO_3$ into Co_3O_4

restrained the crystallization of Co_3O_4 species.

The diffraction peaks of the Co_3O_4 present lower intensity compared to other literature,[22] which can be explained that the Co_3O_4 were primary existed in the form of nanoparticles. Tang et al. revealed that the diffraction peaks intensity of the Co_3O_4 octahedral was stronger than those of the Co_3O_4 nanoparticles.[25] It has been found that the peaks of the Co_3O_4 became broader by the addition of K ions, the reason was that the K ions were highly dispersible in the matrix of the Co_3O_4.[26] But Dean reported that the radius of Ca^+ (r_{Ca2+} =0.099 nm) was much larger than the radius of the $Co^{2+}$and Co^{3+}, so the Ca^+ could not incorporate into the Co_3O_4 lattice.[27] Zhang et al. found that the introduction of Ba to NiO caused NiO diffraction peaks sharply weakened, because $BaCO_3$ could suppress crystal growth of NiO.[28] Therefore, the similar effect could be expected that the introduction of $CaCO_3$ could restrain the crystal growth of the Co_3O_4 in the catalyst samples. In previous studies, many authors believed that the N_2O decomposition activity was obviously influenced by the crystallite size of catalyst.[18]

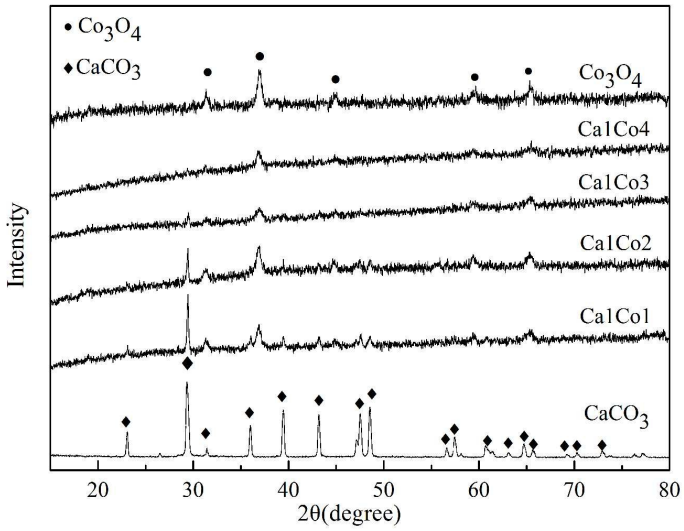

Fig. 1 XRD patterns of different catalysts

3.2 Catalytic activity of $CaCoO_x$ with different compositions for N_2O decomposition

The catalytic performance results of N_2O decomposition over the $CaCoO_x$ with different molar ratio were shown in the **Fig. 2**. It was found that the pure $CaCO_3$ was inactive for N_2O decomposition. By contrast, pure Co_3O_4 showed certain catalytic activity for N_2O decomposition and nearly 100% conversion was achieved at 450 °C. However, it was established by the **Fig. 2** that the addition of Ca into Co_3O_4 could largely improve the catalytic performance for N_2O decomposition. This implied that Co_3O_4 was the active component of $CaCO_3$-Co_3O_4 catalysts, while Ca acted as a promoter. The catalytic performance was strongly dependent on the Ca/Co molar ratio, as the increasing of Ca loading, N_2O conversions were increased sharply. However, excessively increase the loading of Ca could inhibit the catalytic decomposition of N_2O. The Ca1Co2 showed the best catalytic performance of N_2O decomposition, and almost complete conversion of N_2O decomposition could be obtained at 400 °C. But the further increase of Ca/Co molar ratio had a negative effect on the catalytic activity. Thus, Ca which existed in the form of $CaCO_3$ was proposed to be used as the alkaline earth metals for the improvement of the catalytic activity in N_2O decomposition procedure.

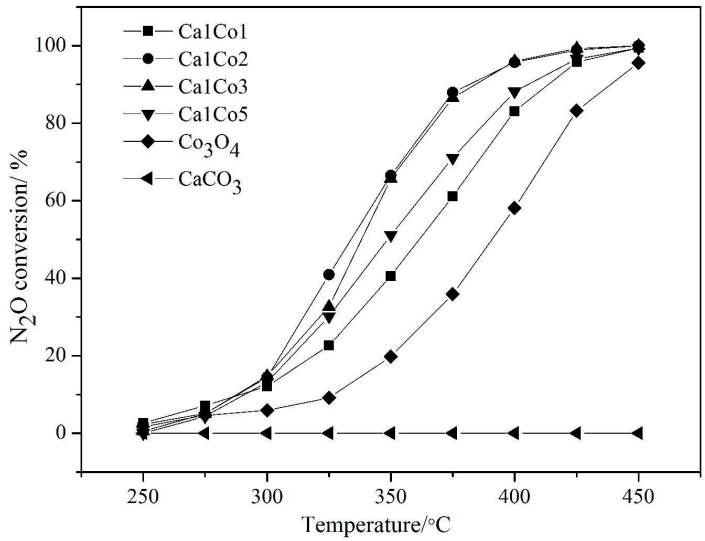

Fig. 2 The N_2O conversion over different catalysts with 1000 ppm N_2O/Ar.

It was established that the oxygen desorbing from active sites was the rate-determining step,[22] thus the N_2O decomposition activity strongly depended on the

oxygen desorption capability. However, the process of oxygen desorption could be inhibited in the presence of excess O_2. It was reported that the water vapor was the other important factor causing the inferior catalytic activity of N_2O decomposition. [6,10] Therefore, it was significant to investigate the effects of O_2 or H_2O on N_2O catalytic decomposition reaction. The effects of O_2 (5 vol. %) or H_2O (3 vol. %) on N_2O decomposition over Ca1Co2 and Co_3O_4 catalysts were illustrated in **Fig. 3**.

As shown in **Fig. 3**, when 5 vol. % O_2 was added to the feed gases, the N_2O decomposition activities of the two samples were both inhibited. However, the catalytic activity of the Ca1Co2 was obviously higher than the pure Co_3O_4. This indicated that the introduction of Ca into Co_3O_4 can significantly enhance the catalytic activity of N_2O decomposition even in the presence of 5 vol. % O_2. As can be seen in **Fig. 3**, with the addition of 3 vol. % water vapor, the catalytic activities were slightly decreased over Ca1Co2 and Co_3O_4 catalysts. It can be seen that the N_2O conversions over Ca1Co2 and Co_3O_4 at 400°C were 95.7% and 58.2% respectively in the absence of H_2O, however, the N_2O conversions decreased to 83.4% and 42.6% respectively when 3 vol. % H_2O was added in the system. The decreased activity in the presence of O_2 or H_2O was mainly caused by the competing adsorption of molecular oxygen, water vapor and reaction gases on the active sites of the catalysts, thus restrained the catalytic decomposition of N_2O.

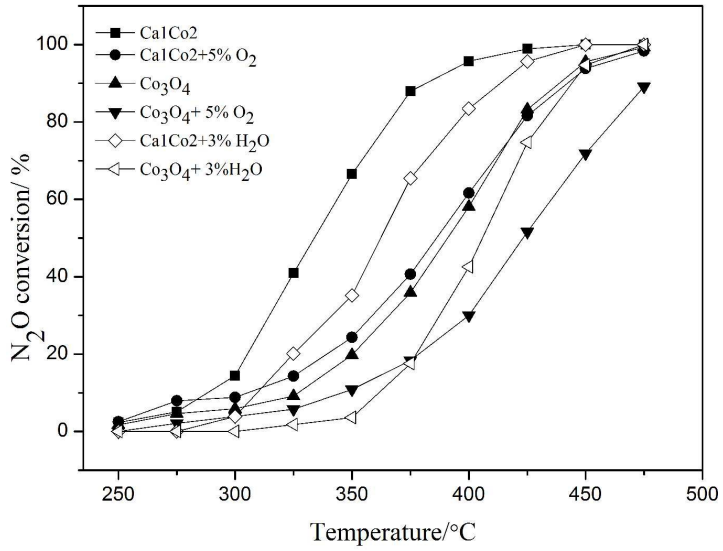

Fig. 3 N_2O conversion over Ca1Co2 and Co_3O_4 catalysts with feed gas of 1000 ppm N_2O/Ar + 5 vol. % O_2 or 1000 ppm N_2O/Ar + 3 vol. %H_2O

3.3 H_2-TPR measurements

It was reported that the reduction of Co^{3+} to Co^{2+} was a very important process for N_2O decomposition over cobalt containing catalysts especially for the desorption of surface oxygen species resulting from the catalytic decomposition of N_2O.[29] In the present study, the H_2-TPR was used to investigate the cobalt species on the Co_3O_4 and $CaCoO_x$ catalysts. As shown in **Fig. 4**, all the samples presented two H_2 consecutive peaks in the temperature of 100 - 500 °C. The first reduction peak at the region of 220 - 320 °C was due to the reduction of Co^{3+} to Co^{2+}, and the second reduction peak in the range of 320 - 470 °C was owing to the reduction of Co^{2+} to Co^0.[30] As can be seen in **Fig. 4**, when the $CaCO_3$ species was added into Co_3O_4, the reduction temperatures of Co^{3+} to Co^{2+} slightly shifted to higher temperature (ΔT_1 = 22 °C), suggesting that the reduction of Co^{3+} was slightly hindered. But the reduction temperatures of Co^{2+} to Co^0 shifted to a lower temperature (ΔT_2 = 43 °C), indicating that reduction of Co^{2+} was improved. It also can be seen that almost similar reduction temperature of Co^{3+} to Co^{2+} was observed over the $CaCoO_x$ catalyst with different Ca/Co molar ratios, it was obvious that the Ca/Co molar ratios showed no visible influence on the reduction behavior of Co^{3+} to Co^{2+}. These results pointed out that the reduction reducibility of Co^{3+} to Co^{2+} on the Co_3O_4 catalyst was decreased by the addition of Ca species. On the contrary, the addition of Ca species into Co_3O_4 catalyst with suitable Ca/Co molar ratios greatly enhanced the catalytic performance of N_2O decomposition. This suggested that the reducibility of Co^{3+} to Co^{2+} was not the key factor for the decomposition of N_2O over the $CaCoO_x$ catalysts in this study.

The **Fig. 4** also showed that the reduction temperature of Co^{2+} to Co^0 shifted to a lower temperature after the addition of Ca species into Co_3O_4 (ΔT_2 = 43 °C), which revealed that the reducibility of Co^{2+} to Co^0 on the Co_3O_4 catalyst was increased by the introduction of Ca species. The increased reducibility of Co^{2+} to Co^0 may offset the decreased reducibility of Co^{3+} to Co^{2+} caused by addition of Ca species into Co_3O_4. Therefore, no negative effects on N_2O decomposition were observed, on the contrary,

the greatly improved effect on N_2O decomposition was observed by the addition of Ca species into Co_3O_4. It is clear that the improved reducibility of Co_3O_4 especially for the reduction of Co^{2+} to Co^0 was conductive to the N_2O decomposition by the addition of Ca species.

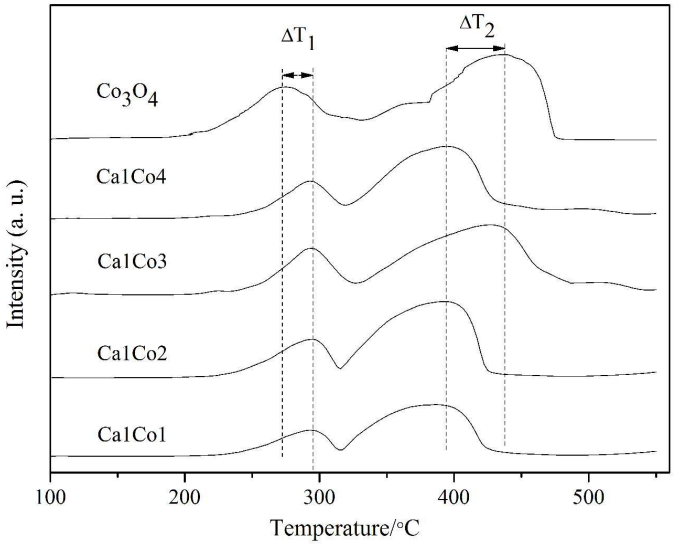

Fig. 4 H_2 -TPR profiles of different catalysts.

3.4 O_2-TPD

It was reported that the oxygen desorbing from active sites was considered as the rate-determining step.[22] The O_2 - TPD experiments were performed over Ca1Co2 and Co_3O_4 to better study the oxygen desorption. As shown in **Fig. 5**, there was an O_2 desorption peak at 150 - 400 °C. The O_2 desorption peak at temperature of 150 - 400 °C was ascribed to the desorption of surface oxygen species such as O_2^- and O^-.[22] The peak can be correlated to the number of oxygen vacancies produced during materials synthesis.[31] From the **Fig. 5**, it can be seen that the Ca1Co2 catalyst presented higher intensity of desorption peak than the pure Co_3O_4. At the same time, the O_2 desorption peak of Ca1Co2 was broader than that of the individual Co_3O_4. The O_2 - TPD analysis indicated that the addition of $CaCO_3$ in the sample can increases the molar amount of desorbed O_2 compared to Co_3O_4. In other words, the Co_3O_4 with the addition of $CaCO_3$ possessed higher amount of O_2-vacancies on the surface.

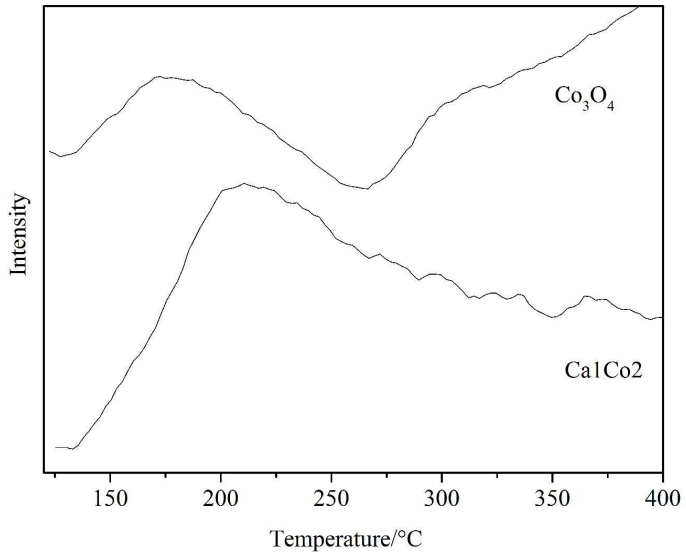

Fig. 5 O_2 -TPD profiles of over Ca1Co2 and Co_3O_4 catalysts

3.5 XPS analysis

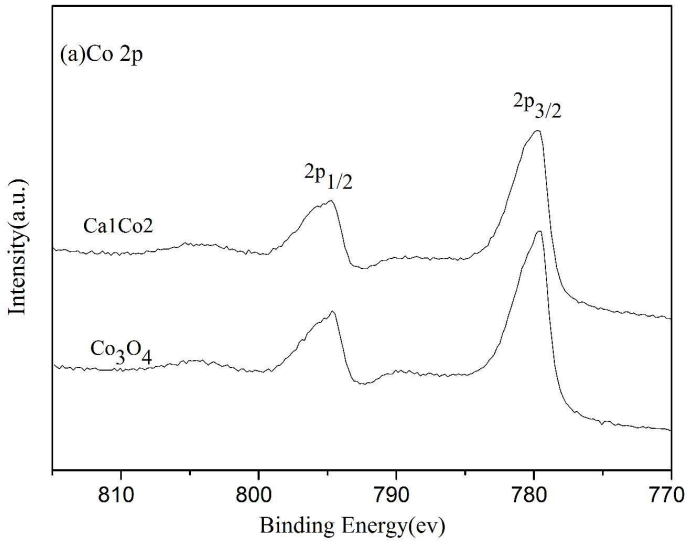

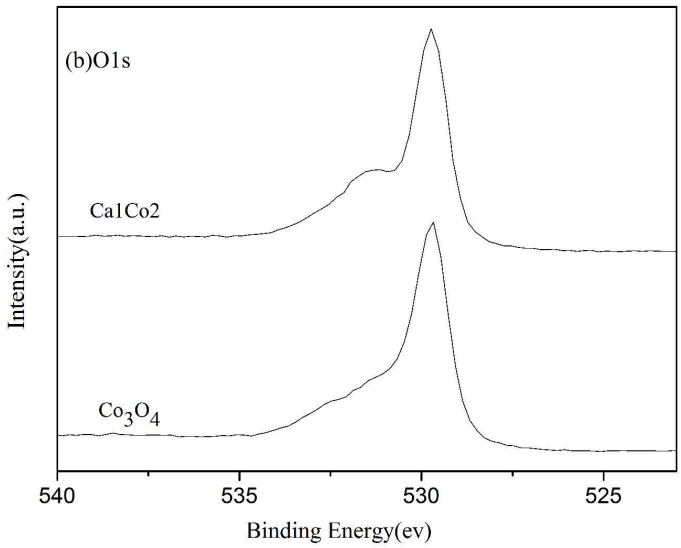

Fig. 6 X-ray photoelectron spectra of: (a) Co2p and (b) O1s core levels of Ca1Co2 and Co_3O_4 catalyst samples.

The XPS was performed to study the oxidation states of various Co species on the surface.[32] The XPS spectra of Co2p of the pure Co_3O_4 and Ca1Co2 were demonstrated in **Fig. 6**. As can be seen in **Fig. 6a**, for the pure Co_3O_4, the Co2p peak can be fitted into two binding energy peak, corresponding to Co2p3/2 (779.7 ev) and Co2p1/2 species (779.7 ev). The addition of Ca showed no observable influence on the valence state of cobalt oxide. At the same time, the spin-orbit splitting (ΔE) of the Co2p peaks (ΔE) was both 15.0 ev, which indicated that the formation of Co_3O_4 spinel phase. The result was in good agreement with the reported results.[33,34] Two small peaks at 789.3 ev and 804.6 ev were also observed in the Co2p region, which were assigned to the Co^{2+} shake-up satellite peaks of Co_3O_4.[34] The analysis results of O1s peak provided the additional information of the two samples. The two contributions arose at 529.7 ev and 531.1 ev on the O1s peak could attribute to the lattice oxygen in oxides and adsorbed oxygen on the catalyst surface that weakly bounded to the catalyst surface.[35,36] According to **Fig. 6b**, it could be seen that the shoulder in the curve of Ca1Co2 was more obvious than that of the pure Co_3O_4. The shoulder position was approximately at 531.1 ev, Liu et al. reported that the higher binding energy shoulder was attributed to the presence of oxygen vacancies or surface oxygen

species.[37] It was clear that there were more surface oxygen or oxygen vacancies in Ca1Co2 than that of the pure Co_3O_4, which may promote the decomposition of N_2O. The results were in accordance with the O_2 - TPD analysis. Zamudio et al. compared the N_2O catalytic activity of $MgCo_2O_4$ prepared by solution combustion synthesis and co-precipitation methods, the catalyst prepared by co-precipitation method provided a higher amount of surface oxygen which showed better N_2O catalytic activity.[38] It was established that the desorption of the surface oxygen that weakly bounded to the surface of catalyst leaded to the formation of anionic vacancies, and the anionic vacancies potentially activate the adsorption and decomposition of N_2O.[39] It was well known that the weaker adsorption oxygen could benefit the surface mobility of oxygen on the catalyst. Because there were larger amount of surface oxygen in the Ca1Co2, therefore, the addition of Ca species enhanced the removal of surface oxygen of Co_3O_4. It was believed that the Ca was conductive to desorption of oxygen, which was the rate determination step in the N_2O decomposition.

3.6 TEM analysis

The further insight into the morphology of the pure Co_3O_4 and Ca1Co2 catalyst were revealed by TEM characterization. Typical low magnification TEM images were presented in **Fig. 7a** and **Fig. 7b**, it can be seen that the Co_3O_4 particles are all nanoparticles with a diameter size of approximately 10-50 nm. The particle size distribution were displayed in the **Fig. 7a′** and Fig**. 7b′**, the mean diameter size (22.8 nm) of Ca1Co2 (22.88nm) were smaller than that of the pure Co_3O_4 (26.18 nm). This result showed that the addition of Ca species into Co_3O_4 could decrease the average size of the samples. Moreover, the **Fig. 7a** illustrated that the addition of Ca species could also improve the dispersion of Co_3O_4 compared to the pure Co_3O_4. The previous work revealed that the dispersity of the cobalt oxides in the cobalt and cerium binary oxide sample is higher than in the individual cobalt oxide, the addition of CeO_2 into the cobalt oxide can prevent the sintering of cobalt oxide microcrystals.[40] Furthermore, Zhou et al. reported that the introduction of CeO_2 to metal oxides such as the Co_3O_4, CuO, and NiO could provide higher surface area and prevented the metal oxides from agglomeration.[41,42] Qiao et al. suggested that the addition of Ca species can increase

the dispersity of the NiO species on the sample surface.[43] A similar interaction might exist between the Ca and Co_3O_4. Due to **Fig. 7**, it was proved that the excellent dispersion of Co_3O_4 can contribute to the remarkable N_2O catalytic decomposition activity.

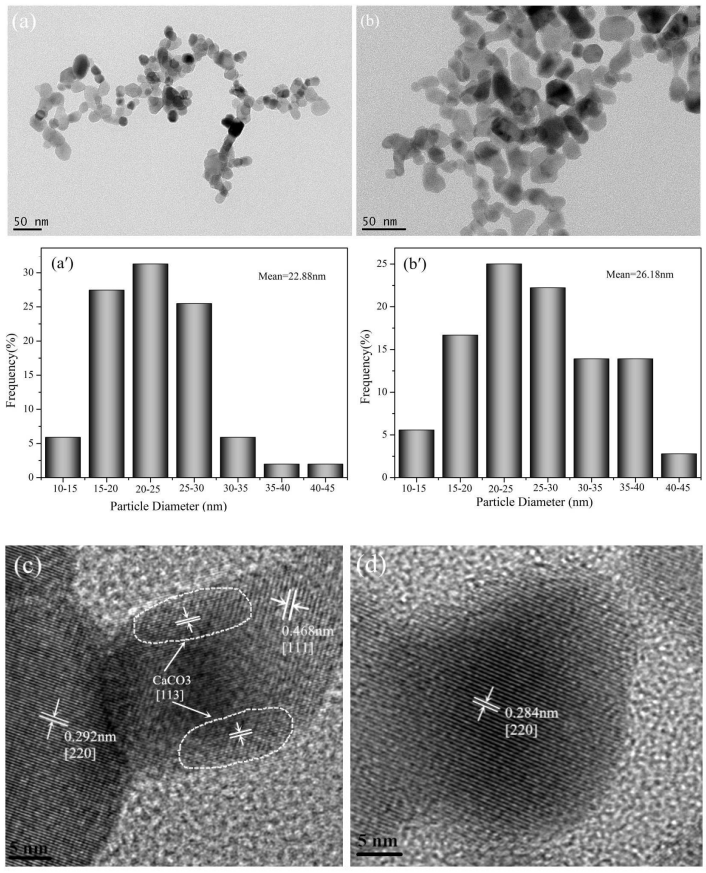

Fig. 7 TEM and HRTEM images of as-synthesized Ca1Co2 (a and c) and Co_3O_4 (b and d). The **Fig. 7a′** and **Fig.7b′** are the size distribution.

Fig.7c and **Fig.7d** showed the high resolution TEM (HR-TEM) images of the pure Co_3O_4 and Ca1Co2 catalysts. The Ca1Co2 lattice spacing of 0.468 nm, 0.292 nm corresponded to the (111), (220) crystal planes of typical Co_3O_4 spinel structure, which was in according with the corresponding XRD pattern. The crystal planes of $CaCO_3$ were found in the cross lattice in the edge of the TEM image of Ca1Co2. The $CaCO_3$ crystal planes were marked by circling. From the **Fig. 7c**, it can be observed that the lattice spacing of d = 0.23nm - 0.25nm corresponds to facets of the $CaCO_3$. It belonged to 113 lattice plane of the $CaCO_3$.[44] The lattice spacing of (220) crystal

plane of the pure Co_3O_4 was corresponding to 0.284 nm. From all the HR-TEM pictures of the pure Co_3O_4, no any (111) crystal planes of Co_3O_4 was observed. It could be speculated that the Ca could promote the lattice of (111) crystal planes exposing on the catalysts surface.

From the results discuss above, it is clear that the addition of $CaCO_3$ into Co_3O_4 catalyst influenced the reducibility of the catalyst. The H_2-TPR results also confirmed that the addition of $CaCO_3$ into Co_3O_4 could promote the reduction of Co^{2+} to Co. It has been reported that active sites with better reducibility exhibit higher activities in N_2O decomposition.[45] Therefore, it could be concluded that the CaxCoy catalysts with stronger reducibility show higher activities than the pure Co_3O_4. Simultaneously, it has been reported that the higher amount of oxygen sites on the surface of catalyst contributed to the N_2O decomposition.[38] From **Fig. 6b**, it could be easily seen that the Ca1Co2 exhibited higher amount of surface oxygen than that of the individual Co_3O_4. The similar phenomenon was also observed in the O_2-TPD. As a consequence, the introduction of $CaCO_3$ into Co_3O_4 enhanced the catalytic activity of N_2O decomposition.

3.7 Steady-state kinetics studies

The rates of N_2O decomposition (r_m) were calculated using the following equation:

$$r_m = \left(\frac{V}{m_{cat}}\right)\left([N_2O]_{in} - [N_2O]_{out}\right)$$

Where V was the real volume flow rate, m_{cat} was the amount of the catalyst, $[N_2O]_{in}$ and $[N_2O]_{out}$ were respectively the inlet and outlet N_2O concentrations. The rate of N_2O decomposition were calculated at temperatures of 400 °C and 450 °C, the concentration of N_2O was varied from 600 to 1400 ppm. The calculated rates were presented in **Fig. 8**, it can be seen that the rate of N_2O decomposition over Ca1Co2 and Co_3O_4 increased linearly with the increase of N_2O concentration. This suggested that the N_2O decomposition was a first order reaction. The result was in good agreement with conclusions of other studies.[36,43]

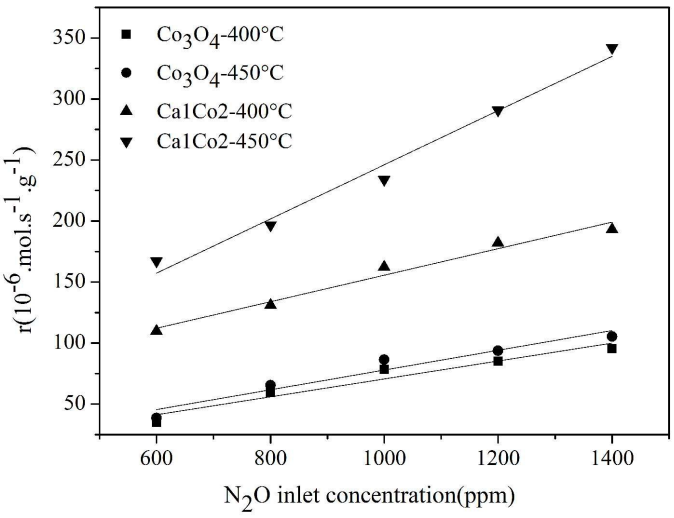

Fig. 8 Dependence of N_2O conversion rate on N_2O inlet concentration on Ca1Co2 and Co_3O_4 catalysts at 400 °C and 450 °C.

The activation energy (Ea) was calculated using the Arrhenius equation:

$$k = A\exp\left(\frac{-Ea}{RT}\right)$$

Where k was the first-order rate constant, T was the reaction temperature, A was the pre-exponential factor, Ea was the activation energy. The plot of ln(k) versus 1/T was drawn according to the data obtained from steady-state reaction.

The Arrhenius plots of N_2O decomposition over Ca1Co2 and Co_3O_4 catalyst were shown in **Fig. 9**. The addition of Ca species into the Co_3O_4 showed a significant effect on the activation energy. It is clear that the activation energy of the Ca1Co2 (Ea=17.84kJ/mol) was much lower than that of the Co_3O_4 (Ea=43.21kJ/mol), which indicated that the existence of Ca species on the surface could greatly reduce the activation energy in the decomposition of N_2O. It was thus indicated that the addition of Ca species into Co_3O_4 could offer more active species during N_2O catalytic decomposition. According to previous discussion that Co_3O_4 was the active sites for N_2O decomposition over the Ca1Co2 catalyst. Based on the XRD and TEM results, the introduction of the Ca species can increase the dispersion of the Co_3O_4. Compared with Co_3O_4, the Ca1Co2 catalyst presented a better dispersion of metal species in

catalyst, which may provide more active sites to take part in the reaction of the N_2O decomposition. It was established that the adsorption of the N_2O and desorption of oxygen were the rate-determining step. Due to the large difference of activation energy between the Ca1Co2 (Ea=17.84 kJ/mol) and the Co_3O_4 (Ea =43.21kJ/mol), it might imply that the N_2O-adsorptive property was an essential feature that can affect the rate of N_2O decomposition. Kondratenkoa et al. reported that N_2O adsorption should be taken into consideration for catalytic N_2O decomposition.[46] The lower activation energy over the Ca1Co2 catalyst, suggesting that the addition of Ca species may accelerate the N_2O adsorbing on the active sites of Co_3O_4 catalyst.

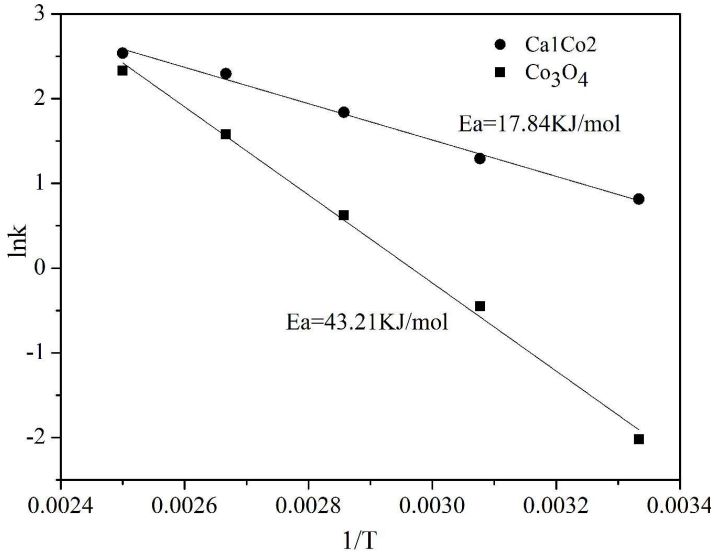

Fig. 9 Arrhenius plot of N_2O decomposition on Ca1Co2 and Co_3O_4 catalysts

Conclusion

The addition of $CaCO_3$ into Co_3O_4 could significantly enhance the catalytic performance for N_2O decomposition. The species of Ca is mainly presented in the form of $CaCO_3$ in all $CaCoO_x$ samples. The addition of $CaCO_3$ into the Co_3O_4 catalyst could suppress the crystal growth of Co_3O_4 and promote the reduction of Co^{2+} to Co, which can benefit the N_2O decomposition. Moreover, the Co_3O_4 doped with Ca species presented smaller particle diameter and provided higher amount of surface oxygen. The kinetics studies revealed that the N_2O catalytic decomposition reaction was first-order for the $CaCoO_x$ catalysts. The activation energy for Ca1Co2 catalyst

(Ea=17.84kJ/mol) was lower than the pure Co_3O_4 (Ea=43.21kJ/mol), suggesting that the addition of Ca enhanced the catalytic decomposition of N_2O.

Acknowledgments

This work is supported by the National Natural Science Foundation of China (No. 21307047, No.U1137603).

References

1 H. B. Zhou, P. L. Hu, Z. Huang, F. Qin, W. Shen and H. L. Xu, Ind. Eng. Chem. Res., 2013, **52**, 4504-4509.

2 P. Kustrowski, L. Chmielarz, A. Rafalska-Łasocha, B. Dudek, A. Pattek-Janczyk and R. Dziembaj, Catal. Commun., 2006, **7**, 1047-1052.

3 L. Obalová, K. Karásková, K. Jirátová and F. Kovanda, Appl. Catal. B., 2009, **90**, 132-140.

4 T. J. Wallington and P. Wiesen, Atmos Environ., 2014, **94**, 258-263.

5 M. A. Zamudio, S. Bensaid, D. Fino and N. Russo, Ind. Eng. Chem. Res., 2011, **50**, 2622-2627.

6 R. Amrousse and T. Katsumi, Catal. Commun., 2012, **26**, 194-198.

7 S. Imamura, R. Hamada, Y. Saito, K. Hashimoto and H. Jindai, J Mol Catal A-Chem., 1999, **139**, 55-62.

8 T. N. Angelidis and V. Tzitzios, Ind. Eng. Chem. Res., 2003, **42**, 2996-3000.

9 J. P. Dacquin, C. Dujardin and P. Granger, J.Catal. , 2008, **253**, 37-49.

10 C. Ohnishi, K. Asano, S. Iwamoto, K. Chikama and M. Inoue, Catal. Today, 2007, **120**, 145-150.

11 K. S. Chang, H. Song, Y. S. Park and J. W. Woo, Appl. Catal. A., 2003, **273**, 223-231.

12 M. F. Fellah and I. Onal, Catal. Today., 2008, **137**, 410-417.

13 A. H. Øygardena and J. Pérez-Ramírez, Appl. Catal. B. , 2006, **65**, 163-167.

14 N. Liu, R. D. Zhang, B. H. Chen, Y. P. Li and Y. X. Li, J. Catal., 2012, **294**, 99-112.

15 F. Kapteijn, J. Rodriguez-Mirasol and J. A. Moulijn, Appl. Catal. B, 1996, **9**, 25 - 64.

16 R. Amrousse, A. Tsutsumi, A. Bachar and D. Lahcene, Appl. Catal. A, 2013, **450**, 253-260.

17 L. Yan, T. Ren, X. L. Wang, Q. Gao, D. Ji and J. S. Suo, Appl. Catal. B, 2003, **45**, 85-90.

18 B. M. Abu-Zied, S. A. Soliman and S. E. Abdellah, J. Ind. and Eng. Chem., 2015, **21**, 814-821

19 L. Yan, T. Ren, X. L. Wang, D. Ji and J. S. Suo, Catal. Commun, 2003, **4**, 505-509.

20 W. Piskorz, F. Zasada, P. Stelmachowski, A. Kotarba and Z. Sojka, Catal. Today, 2008, **137**, 418-422.

21 G. Maniak, P.Stelmachowski, J.J.Stanek, A.Kotarba and Z. Sojka, Catal. Commun. 2011, **15**, 127-131.

22 L. Xue, C. B. Zhang, H. He and Y. Teraoka, Appl. Catal. B, 2007, **75**, 167-174.

23 G. Maniaka, P. Stelmachowski, A. Kotarba, Z. Sojka, V. Rico-Pérez and A. Bueno-López, Appl. Catal. B., 2013 , **136-137**, 302-307.

24 V. Gölden, S. Sokolov, V. A. Kondratenko, E. V. Kondratenko, Appl. Catal. B, 2010, **101**, 130-136.

25 X. F. Tang, J. H. Li and J. M. Hao, Mater. Res. Bull., 2008, **43**, 2912-2918.

26 K. H. Asano, C. Ohnishi, S. Iwamoto, Y. Shioya and M. Inoue, Appl. Catal. B, 2008, **78**, 242-249.

27 J. A. Dean, Lange′s handbook of chemistry. 15th ed. New York: McGraw-Hill, 1999: 318-322.

28 F. F. Zhang, X. P. Wang, X. X. Zhang, M. Turxun, H. B. Yu and J. J. Zhao, Chem. Eng. J., 2014, **256**, 365-371.

29 X. Li, H. He, C. Liu, C. B. Zhang and B. Zhang, Environ. Sci. Technol., 2009, **43**, 890-895.

30 C. Y. Ma, Z. Mu, C. He, P. Li, J. J. Li and Z. P. Hao, J Environ Sci., 2011, **23**, 2078-2086.

31 F. Tanja and P. Regina, Appl. Catal. B., 2015, **176–177**, 298-305

32 Y. F. Wang, C. B. Zhang, F. D. Liu and H. He, Appl. Catal. B, 2013, **142-143**,

72-79.

33 T. Warang, N. Patel, R. Fernandes, N. Bazzanella and A. Miotello, Appl. Catal.B, 2013, **132-133**, 204-211.

34 Q. Y. Yan, X. Y. Li, Q. D. Zhao and G. H. Chen, J. Hazard. Mater., 2012, **209-210**, 386-391.

35 J. P. Dacquin, C. Dujardin and P. Granger, J.Catal., 2008, 25, 37-49.

36 Q. Shen, L. D. Li, J. j. Li, H. Tian and Z. P. Hao, J. Hazard. Mater., 2009, **163**, 1332-1337.

37 Q. Liu, L. C. Wang, M. Chen, Y. Cao, H. Y. He and K. N. Fan, J. Catal. , 2009, **263**, 104-113.

38 M. A. Zamudio, S. Bensaid, D. Fino and N. Russo, Ind. Eng. Chem. Res., 2011, **50**, 2622-2627.

39 J. P. Dacquin, C. Lancelot, C. Dujardin, P. DaCosta, G. Djega-Mariadassou, P. Beaunier, S. Kaliaguin, S. Vaudreuil, S. Royer, P. Grange, Appl. Catal. B, 2009, **91**, 596-604.

40 S. O. Soloviev, P. I. Kyriienko and N. O. Popovych. J Environ Sci., 2012, **24**, 1327-1333.

41 H. B. Zhou, Z. Huang, C. Sun, F. Qin, D. S. Xiong, W. Shen and H. L. Xu, Appl. Catal. B, 2012, **125**, 492-498.

42 H. B. Zhou, P. L. Hu, Z. Huang, F. Qin, W. Shen and H. L. Xu, Ind. Eng. Chem. Res., 2013, **52**, 4504-4509.

43 D. S. Qiao, G. Z. Lu, D. S. Mao, Y. Guo and Y. L. Guo, J. Mater. Sci., 2011, **46**, 641-647.

44 L. Obalova and V. Fıla, Appl. Catal. B, 2007, **70**, 353-359.

45 P. F. Xie, Z. Ma, H. B. Zhou, C. Y Huang, Y. H. Yue, W. Shen, H. L. Xua, W. M. Hua and Z. Gao, Microporous Mesoporous Mater., 2014, **191**, 112- 117.

46 E. V. Kondratenkoa, V. A. Kondratenkoa, M. Santiago, J. Pérez-Ramírez, J. Catal., 2008, **256**, 248-258.